Multiple Coulomb Scattering

Single Coulomb scattering

Single Coulomb deflection of a charged particle by a fixed nuclear target.

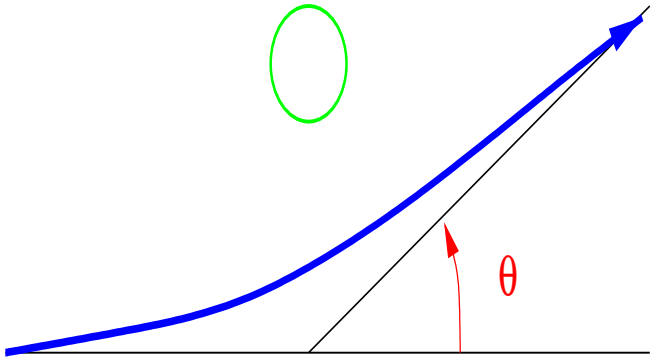

The cross section is given by the Rutherford formula

$$\frac{d\sigma}{d\Omega} = \frac{r_e^2 z_p^2 Z^2}{4} \left(\frac{mc}{\beta p}\right) \frac{1}{\sin^4 \theta/2} \qquad (1)$$

Multiple Coulomb scattering

Charged particles traversing a finite thickness of matter suffer repeated elastic Coulomb scattering. The cumulative effect of these small angle scatterings is a net deflection from the original particle direction.

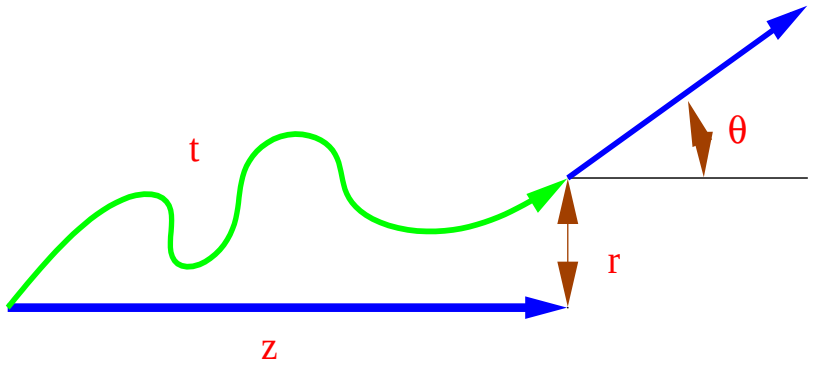

- longitudinal displacement z (or geometrical path length)
- lateral displacement r, Φ
- true (or corrected) path length t
- angular deflection θ, ϕ

The practical solutions of the particle transport can be classified :

- detailed (microscopic) simulation : exact, but time consuming if the energy is not small. Used only for low energy particles.
- condensed simulation : simulates the global effects of the collisions during a macroscopic step, but uses approximations. EGS, Geant3 (both use Moliere theory), Geant4
- mixed algorithms : "hard collisions" are simulated one by one + global effects of the "soft collisions" : Penelope.

Angular distribution

If the number of individual collisions is large enough (> 20) the multiple Coulomb scattering angular distribution is Gaussian at small angles and like Rutherford scattering at large angles.

The Molière theory [Molie48, Bethe53] reproduces rather well this distribution, but it is an approximation.

The Molière theory is accurate for not too low energy and for small angle scattering, but even for this case its accuracy is not too good for very low Z and high Z materials.(see e.g. [Ferna93], [Gotts93])

The Molière theory does not give information about the spatial displacement of the particle, it gives only the scattering angle distribution.

Angular distribution

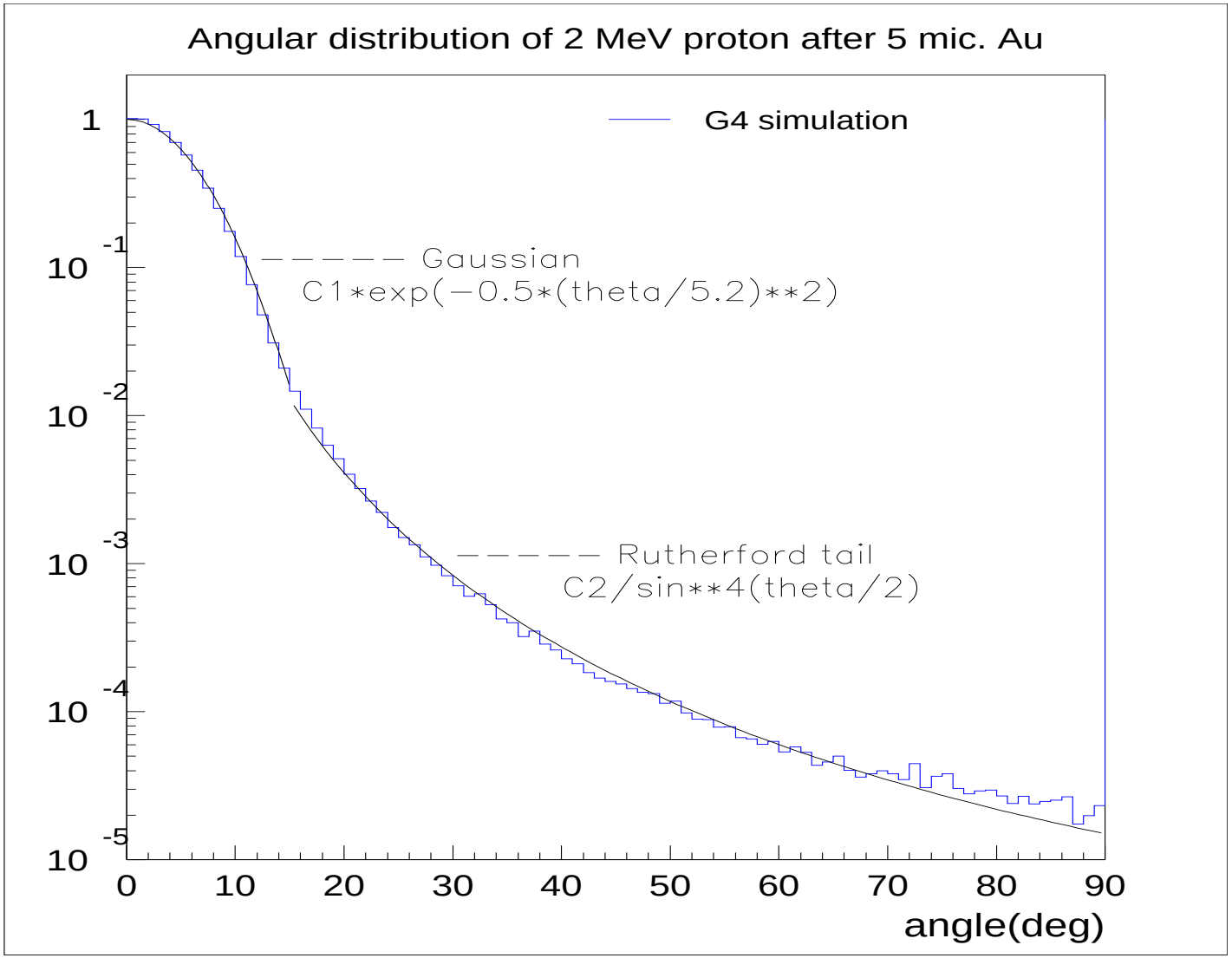

Gaussian approximation

The central part of the spatial angular distribution is approximately

$$P(\theta)\, d\Omega = \frac{1}{2\pi\theta_0^2}\, \exp\left[-\frac{\theta^2}{2\theta_0^2}\right]\, d\Omega$$

with

$$\theta_0 = \frac{13.6\ \text{MeV}}{\beta\, pc} z \sqrt{\frac{l}{X_0}} \left[1 + 0.038 \ln\left(\frac{l}{X_0}\right)\right] \qquad (2)$$

where l/X_0 is the thickness of the medium measured in radiation lengths X_0 ([Highl75],[Lynch91]).

This formula of θ_0 is from a fit to Molière distribution. It is accurate to $\leq 11\%$ for $10^{-3} < l/X_0 < 10^2$

This formula is used very often, but it is worth to note that this is an approximation of the Molière result for the small angle region with an error which can be as big as $\approx 10\%$.

To get a more complete information it is better to start with theory of Lewis which based on the transport equation of charged particles ([Lewis50, Kawra98]).

The MSC model in Geant4 uses model functions to sample angular and spatial distributions after a step.

The functions are choosen in such a way that they give the same moments than the Lewis theory.

The details of the MSC model can be found in the Geant4 Physics Reference Manual.

Transport of charged particles

Let $p(r, d, t)$ denote the probability density of finding the particle at the point $r = (x, y, z)$ moving in the direction of the unit vector $\overrightarrow{d}$ after having travelled a path length t.

The transport is governed by the transport equation :

$$\frac{\partial p(r,d,t)}{\partial t} + \overrightarrow{d} . \overrightarrow{\nabla p(r,d,t)} = n_{at} \int [p(r,d',t) - p(r,d,t)] \frac{d\sigma(\chi)}{d\Omega} d\Omega \quad (3)$$

which can be solved exactly for special cases only.

but this equation can be used to derive different moments of p.

Transport Mean Free Path

$$\frac{1}{\lambda_k} = 2\pi n_{at} \int_{-1}^{1} [1 - P_k(cos\chi)] \frac{d\sigma(\chi)}{d\Omega} d(cos\chi) \qquad (4)$$

$d\sigma(\chi)/d\Omega$ is the differential cross section of the scattering,
$P_k(cos\chi)$ the k-th Legendre polynomial,
n_{at} the nb of atoms per volume.

The first transport mean free path, λ_1, has been calculated by Liljequist et al. for e^- and e^+ in the kinetic energy range 100 eV - 20 MeV in 15 materials [Lilje87], [Lilje90].

For high energy particles (above 10 MeV) the transport mean free path values have been taken from a paper of R.Mayol and F.Salvat ([Mayol97]).

The MSC model in Geant4 uses these values, and when necessary, linearly interpolates the transport cross section, $\sigma_1 = 1/\lambda_1$, in atomic number Z and in the square of the particle velocity, β^2.

The ratio $\kappa = \lambda_1/\lambda_2$ is a slowly varying function of the energy: $\kappa \simeq 2$ for $T \sim$ a few keV, and $\kappa \to 3$ for very high energies (see [Kawra98]).

Hence, a constant value of 2.5 is used in the model.

Transport Mean values

Most of the mean properties of MSC computed in the simulation depend only on the first and second transport mean free paths.

At the end of the true step length, t, the scattering angle is θ.
The mean value of $cos\theta$ is

$$\langle cos\theta \rangle = \exp\left[-\frac{t}{\lambda_1}\right] \tag{5}$$

The variance of $cos\theta$ can be written as

$$\sigma^2 = \langle cos^2\theta \rangle - \langle cos\theta \rangle^2 = \frac{1 + 2e^{-2\kappa\tau}}{3} - e^{-2\tau} \tag{6}$$

where $\tau = t/\lambda_1$ and $\kappa = \lambda_1/\lambda_2$.

The mean value of the geometrical path length (first moment) corresponding to a given true path length t is given by

$$\langle z \rangle = \lambda_1 \left[1 - \exp\left(-\frac{t}{\lambda_1} \right) \right] \tag{7}$$

Eq. 5 -7 are exact results if the differential cross section has axial symmetry and the energy loss can be neglected.

The transformation between true and geometrical path lengths is called the *path length correction*.

This formula and other expressions for the first moments of the spatial distribution were taken from either [Ferna93] or [Kawra98], but were originally calculated by Goudsmit and Saunderson [Gouds40] and Lewis [Lewis50].

The mean lateral displacement can also be calculated relatively easily and accurately. The square of the mean lateral displacement is

$$\langle x^2 + y^2 \rangle = \frac{4\lambda_1^2}{3} \left[\tau - \frac{\kappa+1}{\kappa} + \frac{\kappa}{\kappa-1} e^{-\tau} - \frac{1}{\kappa(\kappa-1)} e^{-\kappa\tau} \right] \quad (8)$$

($\tau = t/\lambda_1$ and $\kappa = \lambda_1/\lambda_2$)

Here it is assumed that the initial particle direction is parallel to the the z axis.

The lateral correlation is determined by the equation

$$\langle x v_x + y v_y \rangle = \frac{2\lambda_1}{3} \left[1 - \frac{\kappa}{\kappa - 1} e^{-\tau} + \frac{1}{\kappa - 1} e^{-\kappa\tau} \right] \qquad (9)$$

v_x and v_y are the components of the direction unit vector $\overrightarrow{d}$.

This equation gives the correlation strength between the final lateral position and final direction.

Energy Dependence

If the energy loss along the step cannot be neglected, Eqs. 5-7 must be modified :

$$\langle cos\theta \rangle = \exp\left[- \int_0^t \frac{du}{\lambda_1(u)} \right] \tag{10}$$

$$\langle z \rangle = \int_0^t \langle cos\theta \rangle_u \; du \tag{11}$$

In order to compute Eqs. 10-11 the t dependence of the transport mean free path must be known. λ_1 depends on the kinetic energy of the particle which decreases along the step. All computations in the model use a linear approximation for this t dependence:

$$\lambda_1(t) = \lambda_{10}(1 - \alpha t) \tag{12}$$

The constant α can be expressed using λ_{10} and λ_{11}, the values of the transport mean free path at the beginning and at the end of the step :

$$\alpha = \frac{\lambda_{10} - \lambda_{11}}{t\lambda_{10}} \tag{13}$$

It is worth noting that Eq. 12 is *not* a crude approximation. It is rather good at low (< 1 MeV) energy. At higher energies the step is generally much smaller than the range of the particle, so is the change in energy.

Using Eqs. 10 - 12 the explicit formula for $\langle cos\theta \rangle$ is :

$$\langle cos\theta \rangle = (1 - \alpha t)^{\frac{1}{\alpha\lambda_{10}}} \tag{14}$$

Mean geometrical path length: $\langle z \rangle$

Using Eqs. 10 - 12 the explicit formula for the geometrical path length z can be written as

$$\langle z \rangle = \frac{1}{\alpha(1+\frac{1}{\alpha\lambda_{10}})}\left[1-(1-\alpha t)^{1+\frac{1}{\alpha\lambda_{10}}}\right] \tag{15}$$

It can easily be seen that for a small step (i.e. for a step with small relative energy loss) the formula of $\langle z \rangle$ gives back the expression 7 :

$$\langle z \rangle = \lambda_{10}\left[1-\exp\left(-\frac{t}{\lambda_{10}}\right)\right] \tag{16}$$

Eq. 15 or 16 gives the mean value of the geometrical step length for a given true step length.

Sampling the geometrical path length: z

The actual geometrical path length is sampled in the model according to the simple probability density function defined for $v = z/t \in [0, 1]$:

$$f(v) = (k+1)(k+2)v^k(1-v) \tag{17}$$

The value of the exponent k is computed from the requirement that $f(v)$ must give the same mean value for $z = vt$ as eq. 15 or 16. Hence :

$$k = \frac{3\langle z \rangle - t}{t - \langle z \rangle} \tag{18}$$

The value of $z = vt$ is sampled using $f(v)$ if $k > 0$, otherwise $z = \langle z \rangle$ is used.

The sampling function: $f(v)$

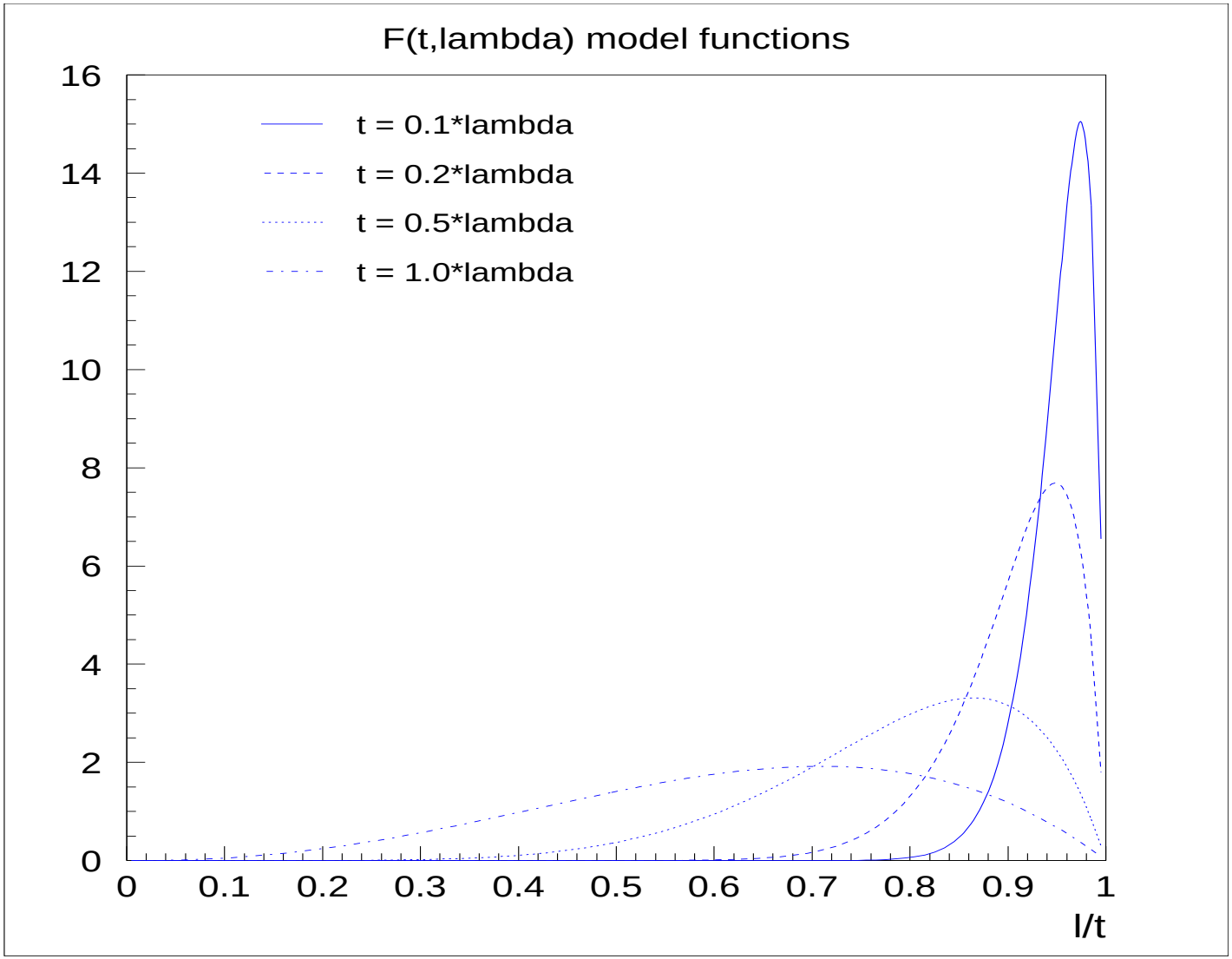

Computing the true path length: t

The $z \to t$ transformation is performed using mean values. The transformation is the inverse of eq. 15 :

$$t(z) = \frac{1}{\alpha}\left[1 - (1 - \alpha w z)^{\frac{1}{w}}\right] \tag{19}$$

where

$$w = 1 + \frac{1}{\alpha\lambda_{10}}$$

If the step is small, the expression is simply (inverse of eq. 16) :

$$t(z) = \langle t \rangle = -\lambda_1 \log\left(1 - \frac{z}{\lambda_1}\right) \tag{20}$$

This transformation is needed when the particle arrives at a volume boundary, causing the step to be geometry-limited.
Then the true path length must be recomputed in order to have the correct energy loss of the particle after the step.

Angular Distribution

$u = cos\ \theta$ is sampled according to a model function $g(u)$:

$$g(u) = p\ [q\ g_1(u) + (1-q)\ g_3(u)] + (1-p)\ g_2(u) \qquad (21)$$

where $0 \leq p, q \leq 1$, and the g_i are simple functions of $u = cos\theta$, normalized over the range $u \in [-1,\ 1]$.

The functions g_i have been chosen as :

$$g_1(u) = C_1 \quad e^{-a(1-u)} \qquad u \in [u_0,\ 1] \qquad (22)$$

$$g_2(u) = C_2 \quad \frac{1}{(b-u)^d} \qquad u \in [-1,\ u_0] \qquad (23)$$

$$g_3(u) = C_3 \qquad u \in [-1,\ 1] \qquad (24)$$

a, b, d, u_0 and the weights p, q are the parameters of the model.
C_i are normalization constants.

It is worth noting that

- at small angle, $g_1(u)$ is nearly Gaussian

$$exp\left[-\frac{\theta^2}{2\theta_0^2}\right] \tag{25}$$

  with $\theta_0^2 = 1/a$

- for large θ, $g_2(u)$ is a Rutherford-like tail if $b \approx 1$ and $d \sim 2$

$$\frac{1}{\sin^4 \theta/2} \tag{26}$$

Determination of the Model Parameters - 1

- $g(u)$ and its first derivative must be continuous at $u = u_0$
- $g(u)$ must give the same $\langle \cos\theta \rangle$ as the theory (eq. 14) :

$$q\ p\ \langle u \rangle_1 + (1-p)\ \langle u \rangle_2\ = [1 - \alpha\ t]^{\ \frac{1}{\alpha \lambda_{10}}} \qquad (27)$$

  where $\langle u \rangle_i$ is the mean value of u computed from the distribution $g_i(u)$.

- The value of u_0 and d has been chosen as

$$u_0 = 1 - \frac{3}{a} \qquad d = 2.40 - 0.027\ Z^{\frac{2}{3}} \qquad (28)$$

  This (empirical) expression is obtained comparing the simulation results to the data of the MuScat experiment [Attw06].

Determination of the Model Parameters - 2

The parameter a was chosen according to a modified Highland formula for the width of the angular distribution.

$$a = \frac{0.5}{1 - cos(\theta_0)} \tag{29}$$

θ_0 is the width of the approximate Gaussian projected angle distribution :

$$\frac{13.6MeV}{\beta cp} z_{ch} \sqrt{\frac{t}{X_0}} \left[1 + 0.105 \ln\left(\frac{t}{X_0}\right) + 0.0035 \left(\ln\left(\frac{t}{X_0}\right)\right)^2 \right]^{\frac{1}{2}} f(Z) \tag{30}$$

where

$$f(Z) = 1 - \frac{0.24}{Z(Z+1)} \tag{31}$$

is an empirical correction factor based on high energy proton scattering data [shen79].

This formula gives much smaller step dependence in the angular distribution and describes the available electron scattering data better than the Highland form.

Angular distribution: $g(cos\theta)$

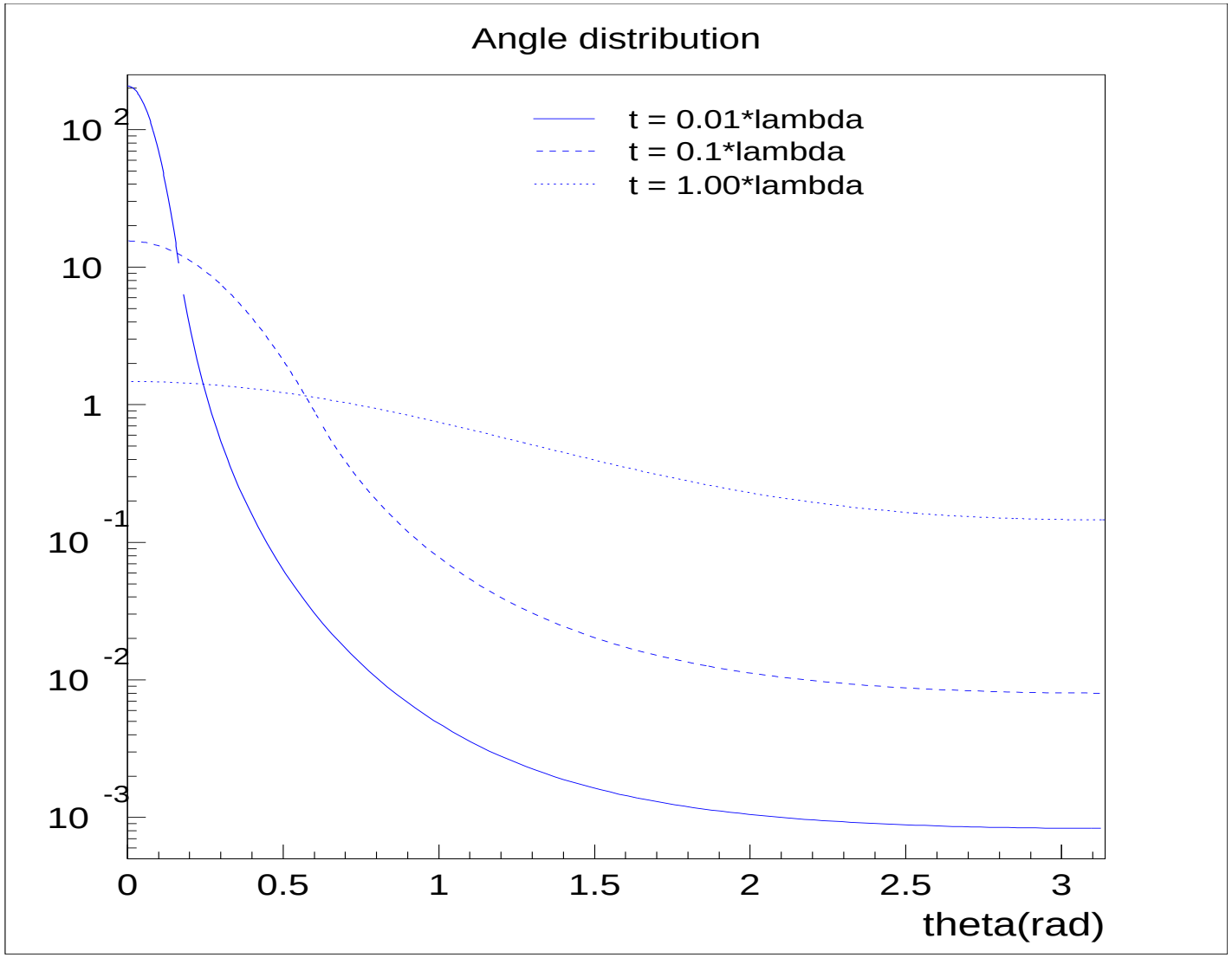

Additional Comments

- In this model there is no step limitation originated from multiple scattering itself.
  However step restrictions are needed for "good boundary crossing".
- With good accuracy, the sum of the 'true' step lengths of the particle does not depend on the length of the steps.
- For heavy charged particles (μ, π, p, etc.) λ_1 is calculated from the electron or positron values with a scaling : λ_1 depends only on the variable $p\beta c$
- In its present form, only mean values of lateral displacement and lateral correlation are computed. However, the model is general enough to incorporate other random quantities in the future.

Nuclear Size Effects

The effect of the finite nuclear size is estimated in Born approximation ([Lilje87]). Then, the scattering cross section can be factorised as

$$\frac{d\sigma(\chi)}{d\Omega} = \frac{d\sigma_B(\chi)}{d\Omega} F(\chi) \tag{32}$$

where $d\sigma_B/d\Omega$ is the Born cross section for a screened point-like nucleus and $F(\chi)$ is the squared nuclear form factor. $F(\chi) \approx 0$ if $\chi > \chi_{max}$ where

$$sin(\frac{\chi_{max}}{2}) = \frac{1}{kR} \tag{33}$$

where k is the particle wave number and R is the nuclear radius. This correction means that $\sigma(\chi)$ decreases, so λ_1 defined by

$$\frac{1}{\lambda_1} = 2\pi n_a \int_{cos\chi_{max}}^{1} [1 - P_1(cos\chi)] \frac{d\sigma_B(\chi)}{d\Omega} F(\chi) d(cos\chi) \tag{34}$$

increases for larger energies.

Nuclear size effects are negligible for low energy particles and they are accounted for in the Born approximation in [Mayol97].

There is no need for extra corrections in the Geant4 model.

MSC Algorithm

Tasks of MSC algorithm are essentially the same for many condensed codes :

1. selection of step length $\longleftarrow$ physics processes + geometry
   MSC performs the $t \rightarrow z$ transformation
2. transport to the initial direction (not MSC business)
3. re-evaluate true step length : $z \rightarrow t$
   sample scattering angle (θ, ϕ)
4. compute lateral displacement (with correlation)
   relocate particle

MSC Algorithm: stage 1

- take the smallest true step length coming from the step limitations given by the physics processes (all but MSC)
  (if needed, apply a Boundary Crossing Algorithm -see below-)
  $t = min(t_{proc1}, t_{proc2}, ..., t_{procn})$
- do the $t \rightarrow z$ transformation $f(z,(t,\lambda)) \Longrightarrow z_{phys}$
  done by AlongStepGetPhysicalInteractionLength() of MSC
- ask step limit z_{geom} from geometry
- take the final (geom.) step size as $z_{step} = min(z_{phys}, z_{geom})$

MSC Algorithm: stage 3

- compute the corresponding true step length $z_{step} \Longrightarrow t_{step}$
  done by AlongStepDoIt() of MSC
- sample θ from the model distribution $g(cos\theta, (t, \lambda))$
  performed by PostStepDoIt() of MSC
- The azimuthal angle ϕ is generated uniformly in the range $[0, 2\pi]$.

MSC Algorithm: stage 4

- After the simulation of the scattering angle, the lateral displacement is computed using eq. 8.
- Then the correlation given by eq. 9 is used to determine the direction of the lateral displacement.
- Before 'moving' the particle according to the displacement a check is performed to ensure that the relocation of the particle with the lateral displacement does not take the particle beyond the volume boundary.

performed by PostStepDoIt() of MSC

MSC is a ContinuousDiscreteProcess, until now we have seen AlongStepGetPhysicalInteractionLength(), AlongStepDoIt(), PostStepDoIt().

What is the task for PostStepGetPhysicalInteractionLength() ?

It sets only a ForceFlag in order to ensure that PostStepDoIt() is called at every step.

Step Limitation Algorithm (1)

The transportation ensures that the particle does not leave a volume without stopping at the boundary. However, this step restriction can be rather weak in big volumes and this fact can result a not very good angular distribution after the volume.

At the same time, there is no similar step limitation when a particle enters a volume and this fact does not allow a good backscattering simulation for low energy particles. Low energy particles penetrate too deeply into the volume in the first step and then - because of energy loss - they are not able to reach again the boundary in backward direction. The backscattering rate is underestimated.

Step Limitation Algorithm (2)

At the start of a track or after entering in a new volume, restrict the step size :

$$t = f_r \cdot max\{r, \lambda_1\} \tag{35}$$

r is the range of the particle, f_r is a constant ($f_r \in [0, 1]$)

(taking the max of r and λ_1 is an empirical choice)

A lower limit is given for the step size :

$$tLimitMin = max\left[\frac{\lambda_1}{nstepmax}, \lambda_{elastic}\right] \tag{36}$$

with nstepmax = 25

$\lambda_{elastic}$ is the mean free path of elastic scattering (see below)

It can be easily seen that this kind of step limitation means a real contraints for low energy particles only.

Step Limitation Algorithm (3)

In order not to allow for a particle to cross a volume in just one step, another limitation is implemented : after entering a volume the step size can not be bigger than

$$\frac{d_{geom}}{f_g} \tag{37}$$

where d_{geom} is the distance to the next boundary (in the direction of the particle) and f_g is a constant parameter.

The choice of the parameters f_r and f_g is a question of compromise between physics and performance.

By default $f_r = 0.02$ and $f_g = 2.5$ are used, but the parameters can be set to any other value in a simple way.

Boundary Crossing Algorithm (1)

This algorithm does not allow 'big' step(s) near a boundary : they cannot be bigger than the mean free path of the elastic scattering.

At end of step(s) the particle scatters according to a single scattering law.

The key parameter of the algorithm is the parameter *skin*.

- $skin = 0$ the algorithm is not active
- $skin > 0$ it is active in a layer of thickness $skin \cdot \lambda_{elastic}$.

The scattering at the end of the step is single or plural and there are no path length correction and no lateral displacement computation.

In other words the program works in 'microscopic mode'.

Boundary Crossing Algorithm (2)

The elastic mean free path can be estimated as

$$\lambda_{elastic} = \lambda_1 \cdot rat\,(T_{kin}) \tag{38}$$

$rat(T_{kin})$ is a simple empirical function computed from the elastic and first transport cross section values of Mayol and Salvat [Mayol97]

$$rat\,(T_{kin}) = \frac{0.001(MeV)^2}{T_{kin}\,(T_{kin} + 10MeV)} \tag{39}$$

T_{kin} is the kinetic energy of the particle.

Boundary Crossing Algorithm (3)

At end of step the number of scatterings is sampled according to the Poissonian distribution with a mean value

$$mean = t/\lambda_{elastic} \tag{40}$$

In the case of plural scattering the final scattering angle is computed by summing the contributions of the individual scatterings.

The single scattering is determined by the distribution

$$g(u) = C\frac{1}{(1+0.5a^2-u)^2} \tag{41}$$

where $u = \cos(\theta)$, a is the screening parameter, C is a normalization constant.

Boundary Crossing Algorithm (4)

The form of the screening parameter is

$$a = \frac{\alpha Z^{1/3}}{\sqrt{(\tau(\tau+2))}} \tag{42}$$

τ is the kinetic energy measured in particle mass units

α is a constant

It can be shown easily that the function $g(u)$ for small scattering angle θ is equivalent to the well known screened Rutherford scattering formula :

$$\tilde{g}(\theta)\ d\Omega = \tilde{C}\frac{\theta\ d\theta}{(a^2+\theta^2)^2} \tag{43}$$

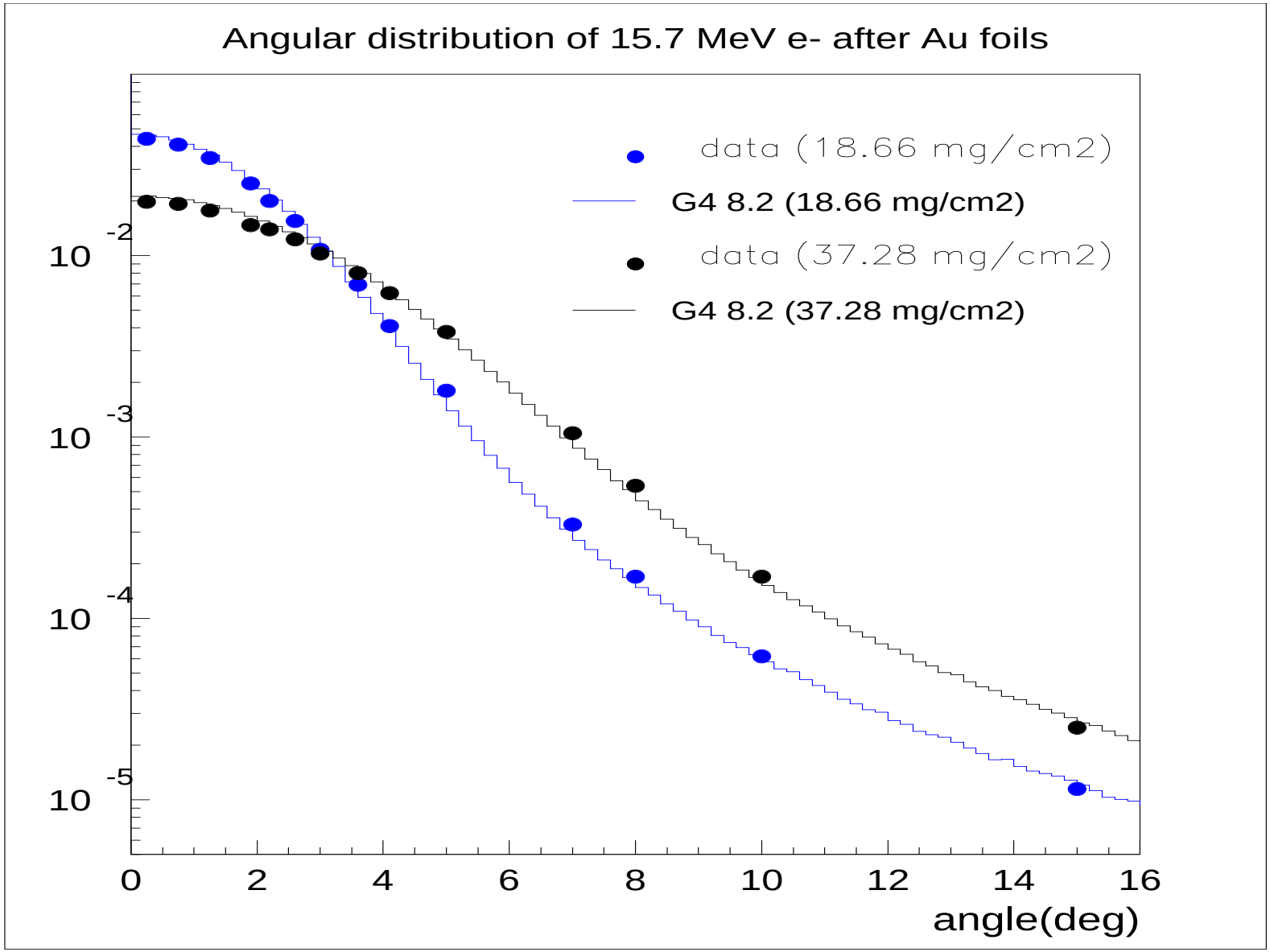
Angular distribution of 15.7 MeV e- after Au foils
data (18.66 mg/cm2)
G4 8.2 (18.66 mg/cm2)
data (37.28 mg/cm2)
G4 8.2 (37.28 mg/cm2)
10^-2
10^-3
10^-4
10^-5
0
2
4
6
8
10
12
14
16
angle(deg)

In Fig.2 the lateral spreading of a 2.5 MeV proton beam is shown after mylar foils of different thicknesses. The spreading is measured in a distance 6.3 mm after the foils, the line representing the experimental data have been taken from [Miche01], the squares are the simulation results. The lateral spreading of the beam is directly connected with the angle distribution of the beam after the mylar absorber, so this result is a benchmark comparison for the angle distribution.

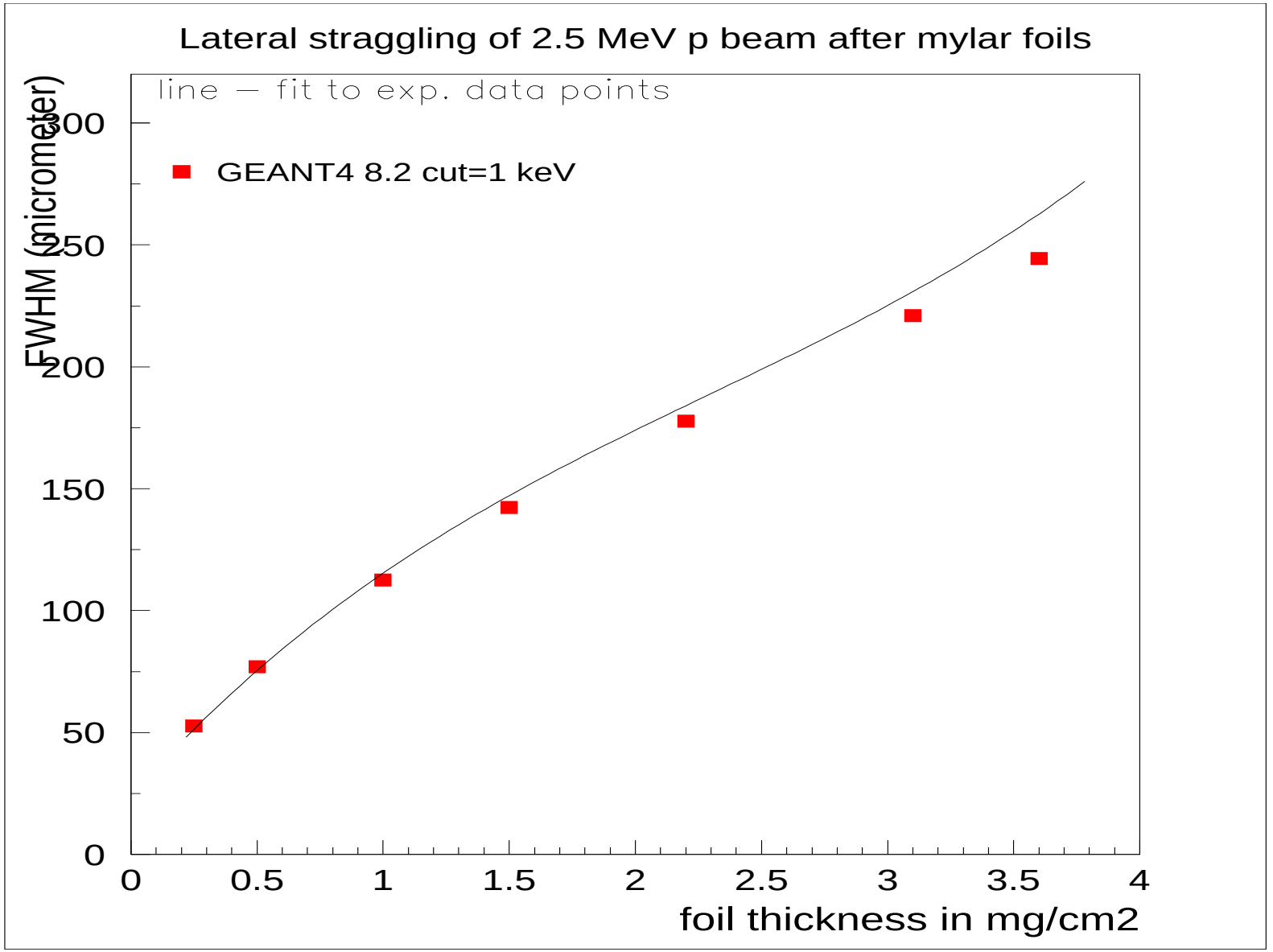
Lateral straggling of 2.5 MeV p beam after mylar foils
line — fit to exp. data points
GEANT4 8.2 cut=1 keV
FWHM (micrometer)
0
50
100
150
200
250
300
0
0.5
1
1.5
2
2.5
3
3.5
4
foil thickness in mg/cm2

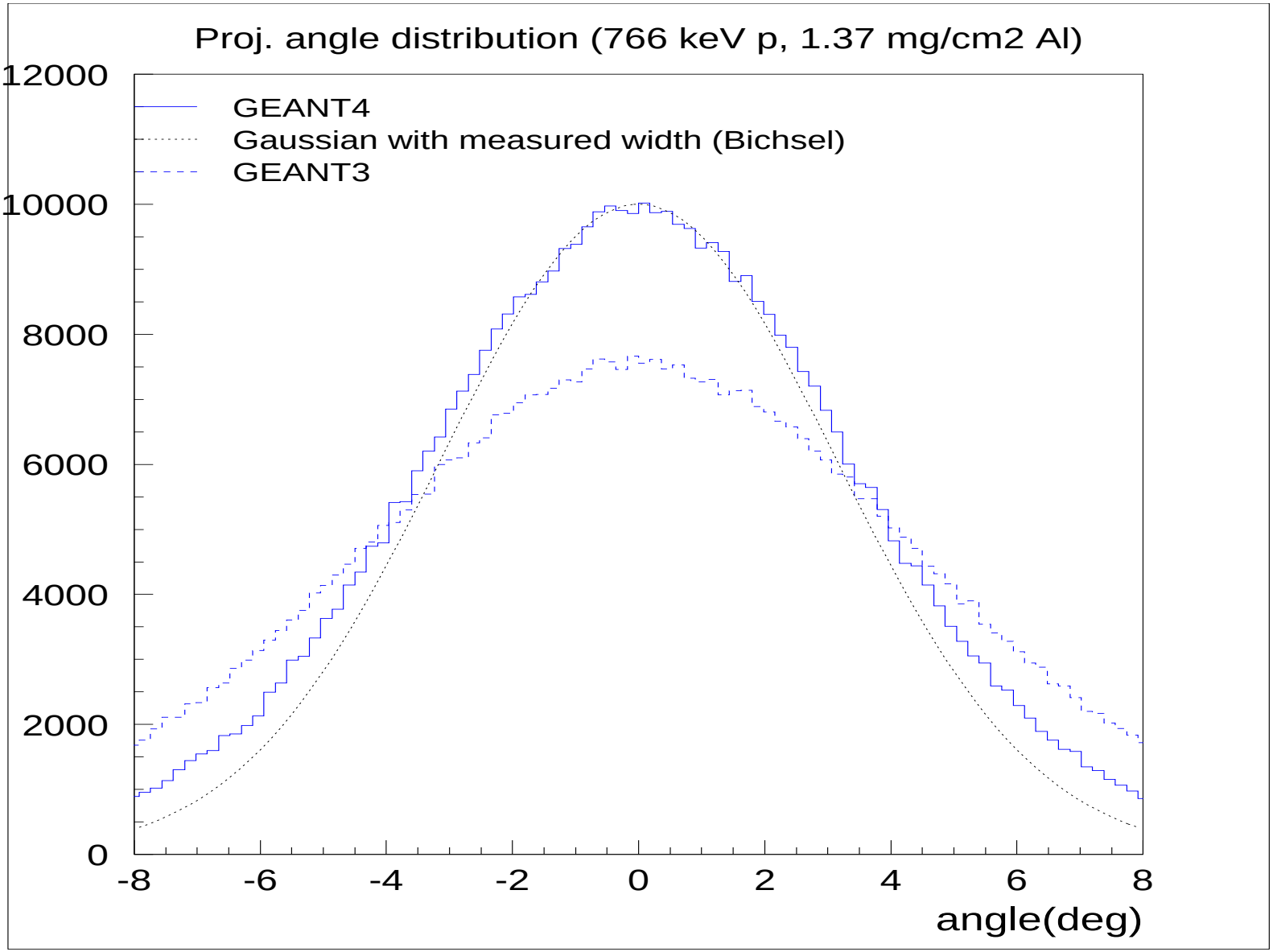
Proj. angle distribution (766 keV p, 1.37 mg/cm2 Al)
GEANT4
Gaussian with measured width (Bichsel)
GEANT3
12000
10000
8000
6000
4000
2000
0
-8
-6
-4
-2
0
2
4
6
8
angle(deg)

Fig. 3 shows the number transmission coefficient T as function of the foil thickness for 1 MeV electrons in aluminium. The thickness is measured in units of the continuous slowing down range, the data originated from different measurements have been taken from the review paper of Seltzer and Berger ([Seltz74]).

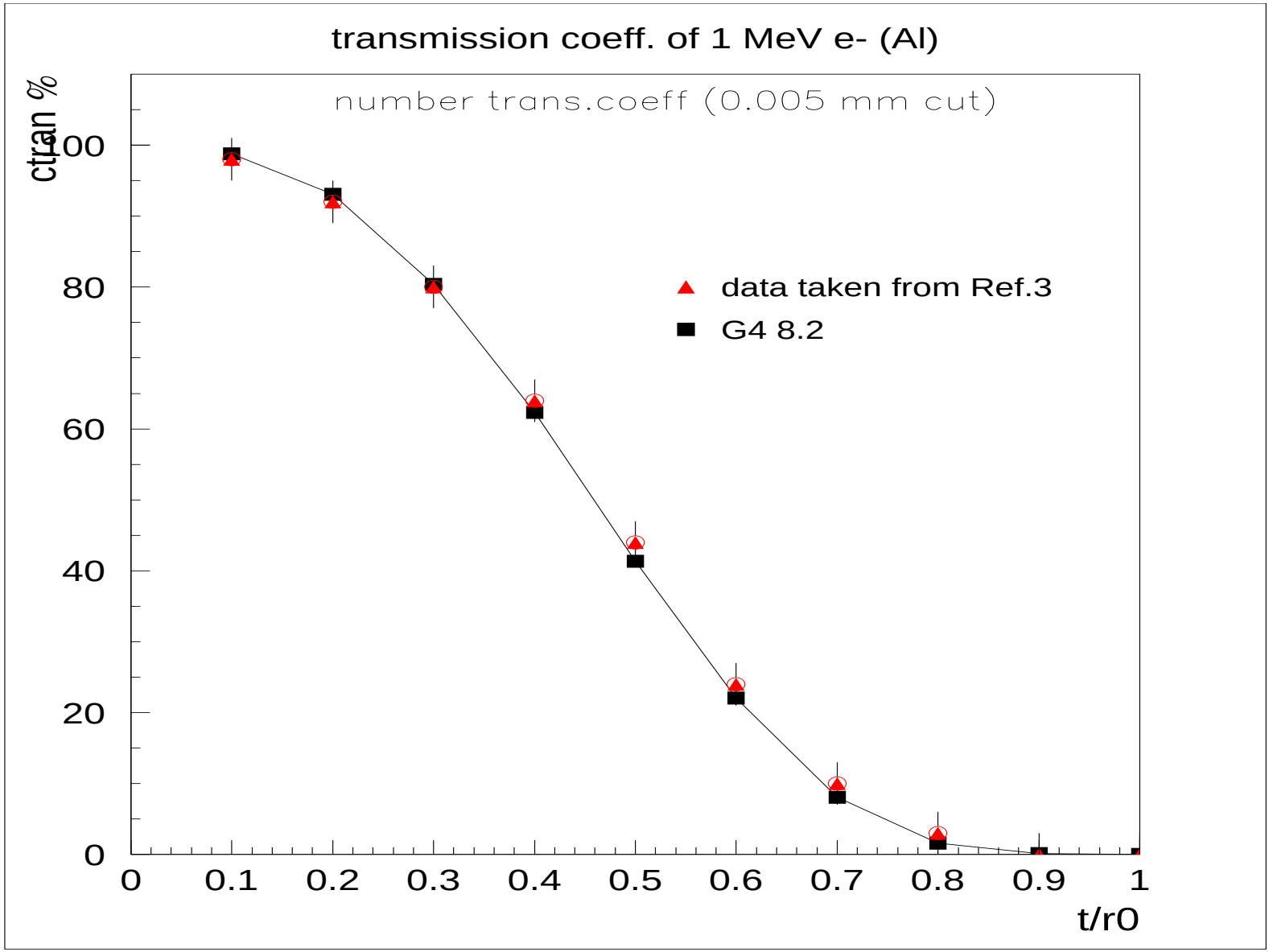
transmission coeff. of 1 MeV e- (Al)
number trans.coeff (0.005 mm cut)
ctran %
100
80
60
40
20
0
0
0.1
0.2
0.3
0.4
0.5
0.6
0.7
0.8
0.9
1
t/r0
data taken from Ref.3
G4 8.2

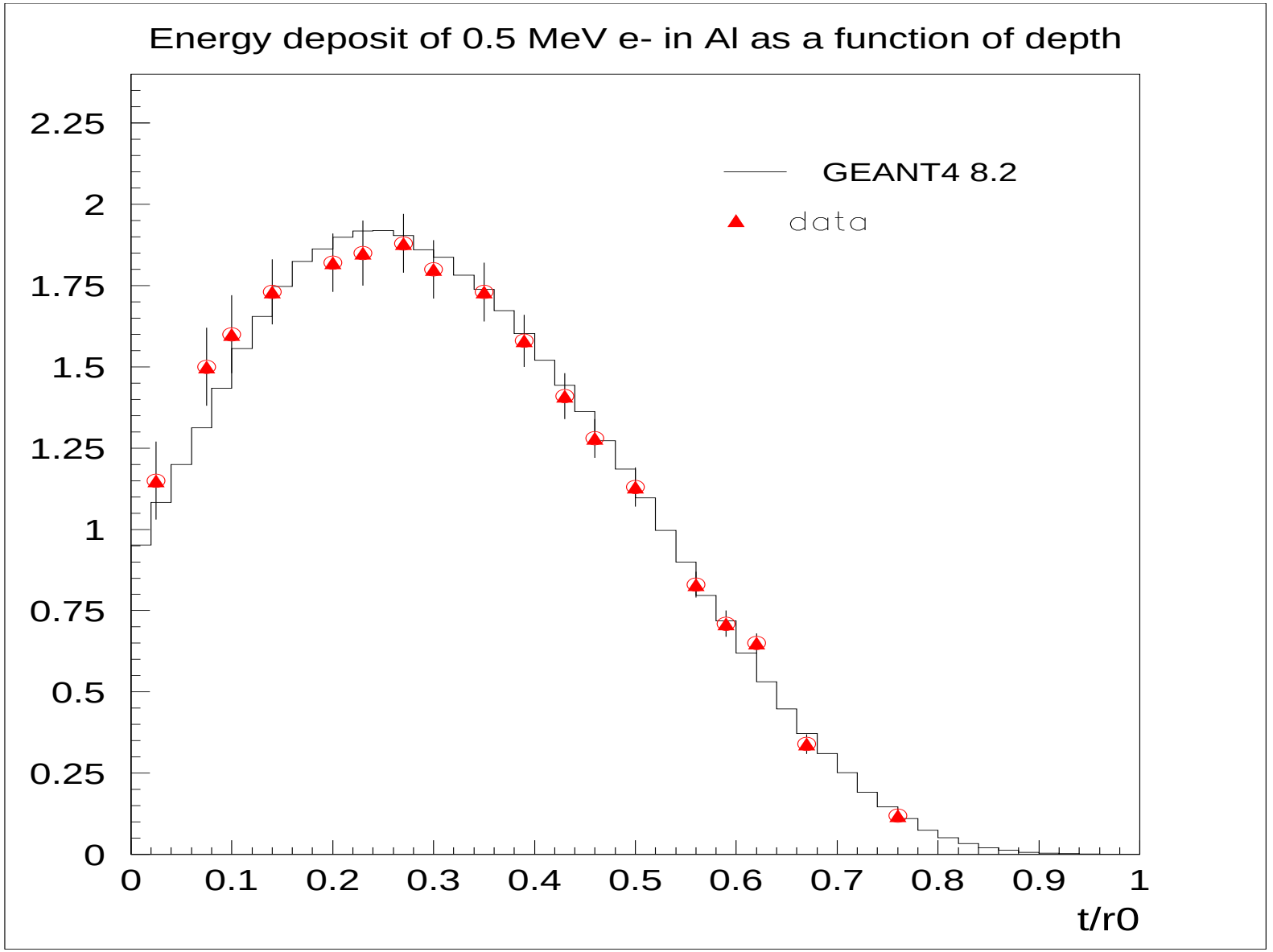
Energy deposit of 0.5 MeV e- in Al as a function of depth
GEANT4 8.2
data
2.25
2
1.75
1.5
1.25
1
0.75
0.5
0.25
0
0
0.1
0.2
0.3
0.4
0.5
0.6
0.7
0.8
0.9
1
t/r0

The energy spectra of 1 MeV electrons transmitted through aluminium foils is shown in Fig. 5. The experimental points are from a measurement of Rester and Derrickson ([Reste70]). The simulation again are quite close to the data.

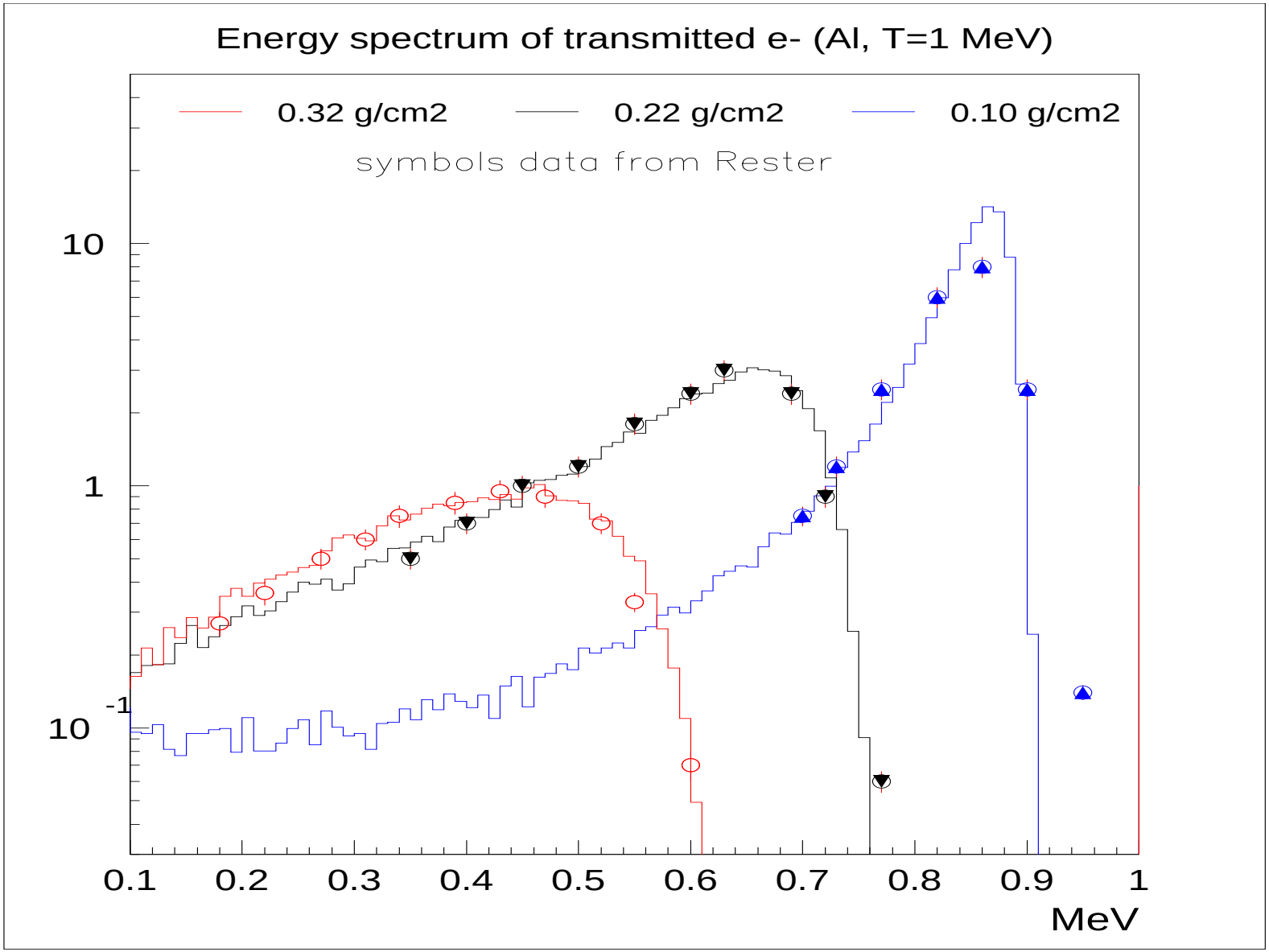
Energy spectrum of transmitted e- (Al, T=1 MeV)
0.32 g/cm2
0.22 g/cm2
0.10 g/cm2
symbols data from Rester
10
1
10 -1
0.1
0.2
0.3
0.4
0.5
0.6
0.7
0.8
0.9
1
MeV

backscattering of low energy electrons The incident beam is 10 electrons of 600 keV entering in 50 μm of Tungsten.
4 electrons are transmitted, 2 are backscattered.

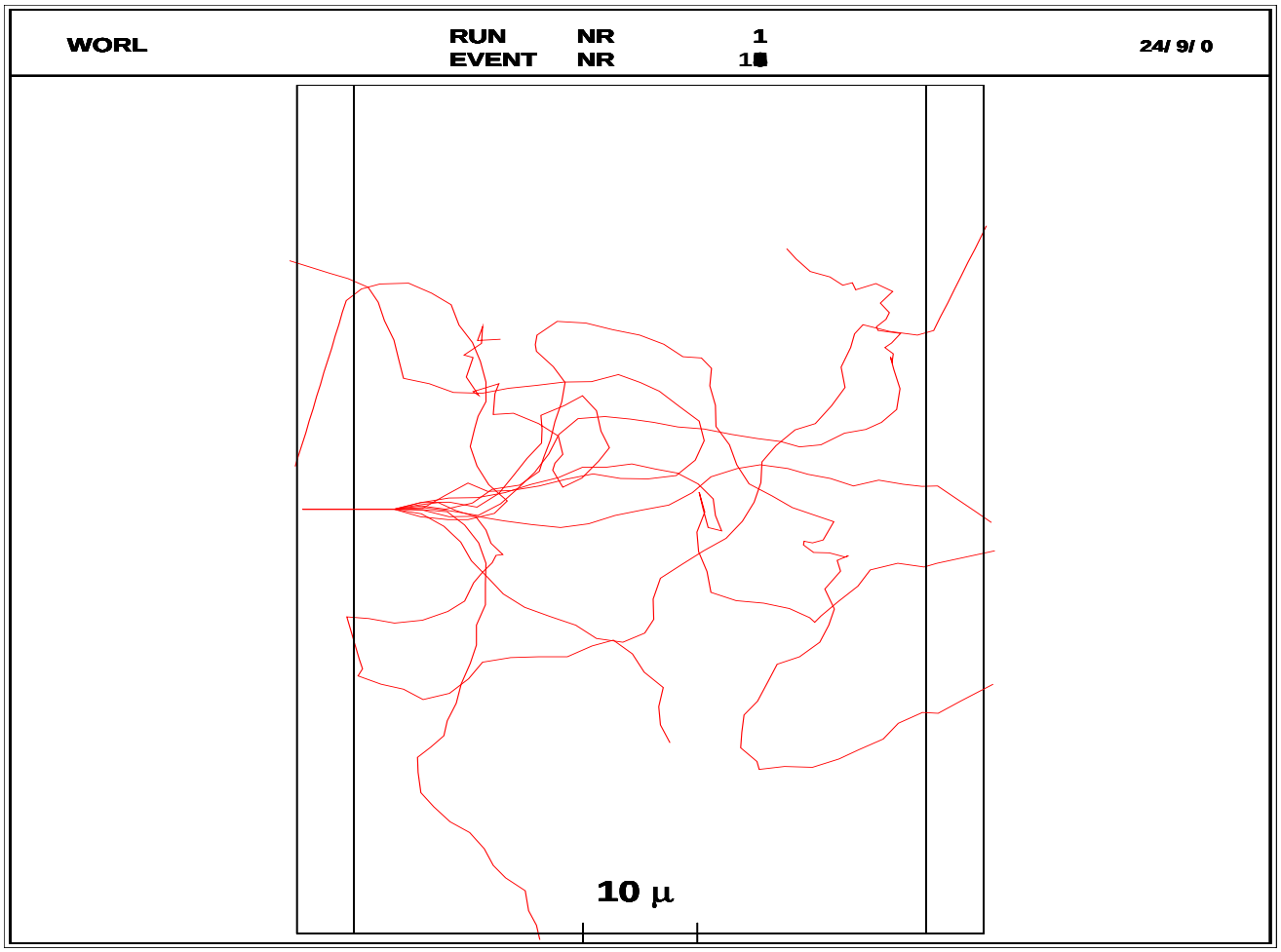

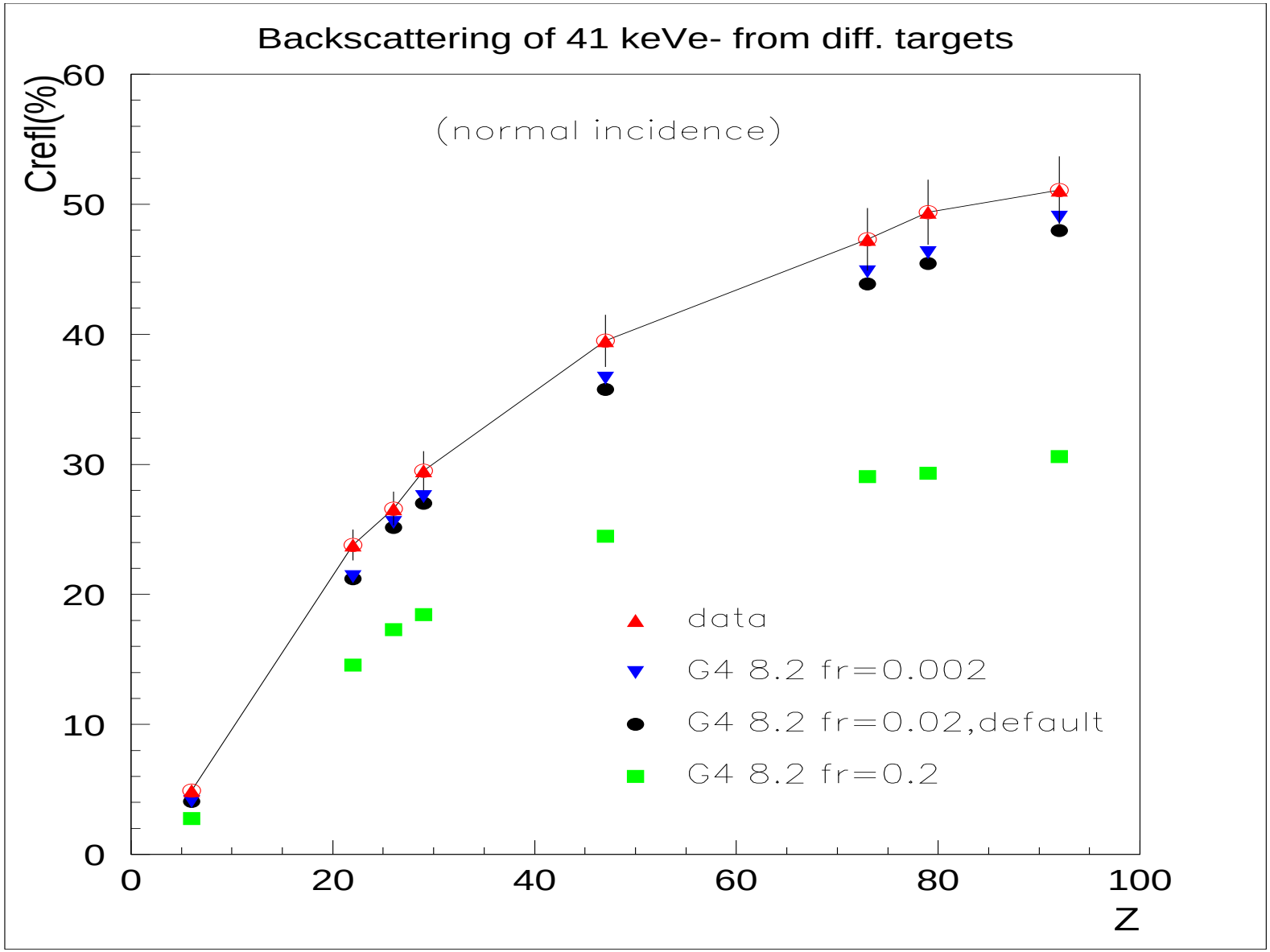
Backscattering of 41 keVe- from diff. targets
(normal incidence)
Crefl(%)
0
10
20
30
40
50
60
0
20
40
60
80
100
Z
data
G4 8.2 fr=0.002
G4 8.2 fr=0.02,default
G4 8.2 fr=0.2

References

[Molie48] Molière, Z. Naturforsch. 3a, 78 (1948)

[Bethe53] H.A.Bethe, Phys. Rev. 89, 1256 (1953)

[Highl75] V.I.Highland, NIM 129, 497 (1975)

[Lynch91] G.R.Lynch and O.I.Dahl, NIM B58,6 (1991)

[Gouds40] S. Goudsmit and J. L. Saunderson. Phys. Rev., 57, 24 (1940).

[Lewis50] H.W.Lewis, Phys. Rev. 78, 526 (1950)

[Kawra98] I.Kawrakow, A.F.Bielajew NIM B142, 253 (1998)

[Ferna93] J.M. Fernandez-Varea et al. NIM B73, 447 (1993)

[Lilje87] D. Liljequist and M. Ismail. J.Appl.Phys., 62, 342 (1987)

[Lilje90] D. Liljequist et al. J.Appl.Phys., 68, 3061 (1990)

[Mayol97] R.Mayol and F.Salvat At.Data and Nucl.Data Tables, 55 (1997)

[Gotts93] B.Gottschalk et al. NIM B74, 467 (1993)

[Seltz74] S.M.Seltzer, M.J.Berger NIM 119, 157 (1974)

[Hunge70] H.J.Hunger, L.Kuchler Phys. Stat. Sol.(a) 56, K45 (1970)

[Reste70] D.H.Rester,J.H.Derrickson J.Appl.Phys. 42, 714 (1970)

[Miche01] C. Michelet et al. NIM, B181, 157 (2001)

[shen79] G.Shen et al. *Phys. Rev. D 20 (1979) 1584.*

[Attw06] D. Attwood et al. *NIM B 251 (2006) 41.*